Proceedings of the Twenty-third (2013) International Offshore and Polar Engineering **www.isope.org**
Anchorage, Alaska, USA, June 30–July 5, 2013

ISBN 978-1-880653-99–9 (Set); ISSN 1098-6189 (Set)

Transverse VIV Response of Piggyback Pipelines with Various Configurations in Ocean Current

Zhipeng Zang[1, 2], *Fuping Gao*[1], *Yongchun Mou*[3] *and Zhibiao Li*[3]

1. Institute of Mechanics, Chinese Academy of Sciences, Beijing, China
2. Key Laboratory of Port, Waterway and Sedimentation Engineering of Ministry of Transport, Nanjing, China
3. PetroChina Planning and Engineering Institute, Beijing, China

ABSTRACT

Transverse vortex-induced vibration of piggyback pipelines under the steady current was physically modeled in a water flume with a hydro-elastic system. In each test, the reduced velocity was gradually increased from 0 to about 16, which covers the typical range of the reduced velocity for pipelines in the field condition. The effects of configuration parameters, including the spacing between the piggyback and the main pipe (G/D), the position angle of the piggyback to the main pipe (θ) and the mass ratio (m^*) on the vibration amplitude and frequency are investigated. The critical reduced velocity for onset of VIV is also examined.

KEY WORDS: Transverse VIV, piggyback pipelines, gap ratio, position angle, mass ratio.

INTRODUCTION

The Piggyback pipeline which comprises a primary trunkline and a secondary smaller flowline, is a special type of submarine pipelines used in the offshore oil and gas engineering. Comparing with the isolated pipeline, the flow around piggyback pipelines is more complicated due to the existence of the piggyback. The vortex shedding from the main pipe may be suppressed by the piggyback in some cases, bringing alleviation of Vortex-Induced Vibrations (VIVs) of the pipeline system. Therefore, investigations on the VIV response of piggyback pipelines with various configurations are of importance for pipeline designs and operations.

The hydrodynamic forces and flow characteristics of piggyback pipelines were mainly studied in past two decades with both experimental and numerical methods. Li and Zhang (1994) measured the hydrodynamic forces and established the empirical relationship between force coefficients of piggyback pipelines and the KC number under combined waves and currents. Chung and Conti (1994) conducted a series of tests and found that the pipe wound with power cables and with perforated shroud can reduce effectively the vortex shedding intensity and hydrodynamics forces compared with a bare pipe. Kalahatgi and Sayer (1997) found that the existence of the piggyback increases the drag force on the pipeline system by 50%-100%. Kamarudin et al (2006) numerically studied the hydrodynamic characteristics of piggyback pipelines mounted on a seabed and found that the Equivalent Diameter method extensively adopted in engineering design may underestimate the forces on the bundle. Zhao et al (2007a) developed a numerical model and simulated flow fields and forces around two circular cylinders of different diameters at $Re = 5\times10^4$. In Zhao et al (2007b), piggyback pipelines near a plane seabed were further simulated in the steady current at $Re = 2\times10^4$. The effects of the gap ratio (e/D, e = gap between the main pipe and the plane wall, D = diameter of the large pipe) and the spacing ratio (G/D, G = spacing between two pipes) on wake flow fields and force coefficients of piggyback pipelines were investigated.

There were few efforts reported on the VIV response of piggyback pipelines. An et al (2008) numerically simulated the transverse VIV of two circular cylinders of different diameters in the tandem arrangement at the reduced velocity $V_R = 8$ ($V_R = U/f_nD$, U = flow velocity, f_n = natural frequency in water.). It was found that the larger cylinder experiences the largest vibration amplitude and the largest force coefficient in the case of $G/D = -1.5$. Rahmanian et al (2012) numerically studied the two-degree-of-freedom VIV of two mechanically coupled circular cylinders at $V_R = 8$. The highest vibration amplitudes in both transverse and in-line directions occur at $\theta = 67.5^o$ for $G/D = 0.1$. The minimum transverse vibration amplitude occurs at $\theta = 112.5^o$ for $G/D = 0.3$. Zang et al (2012) measured wake flow fields around piggyback pipelines near a plane wall with the PIV technique. The suppression of vortex shedding from the main pipe by the piggyback was investigated with the swirling strength analysis and validated with the VIV amplitude ($V_R = 6$). All above studies simulated VIV of piggyback pipelines at a certain constant reduced velocity. However, the overall VIV response in the velocity range throughout the service life of submarine pipelines has not been well investigated.

This paper presents a continuing work of the study on the VIV response of piggyback pipelines conducted in Zang et al (2012). The steady current was accelerated evenly from 0 to 0.8m/s, rather than at a certain constant velocity. The corresponding reduced velocity ranges from 0 to about 16, which covers the typical range of the reduced velocity for submarine pipelines in field conditions. The effects of the spacing ratio between two pipes (G/D), the position angle (θ) and the mass ratio m^* (= mass of pipeline / mass of displaced water), on the amplitude and frequency of VIV for piggyback pipelines are investigated. The critical reduced velocity ($V_{R,onset}$) for onset of VIV is also examined.

EXPERIMENTAL SETUP

Transverse VIV of the spanning piggyback pipeline was simulated in a water flume (52.0 m length, 1.0 m width, and 1.5 m depth), at Institute of Mechanics, Chinese Academy of Sciences. The steady current is generated by two paralleled axial-flow pumps and can reach a maximum velocity of 0.8m/s at the water depth of 0.5m in the test. The modeling system for VIV of piggyback pipelines is shown in Fig. 1, which is similar to the one used in Gao et al (2006). The model pipe is attached to the supporting frame by two sliding poles and a set of springs. The sliding poles can move up and down smoothly through four pulley bearings fixed on the inner sides of the supporting frame. The model of the main pipe is made of a plexiglass tube with the outer diameter of D = 80 mm, while the piggyback is made of a plexiglass rod with the diameter of d = 20 mm. The piggyback is installed on the main pipe using a pair of plastic sector plates, through which one can obtain the position angle (θ) ranging in $0^o \sim 180^o$ with the spacing ratio (G/D) ranging from 0 to 0.5. The in-line motion is constrained by two fine copper wires fastened at the two end plates. The length of the pipeline model is L = 980 mm. A laser displacement transducer (LDT) is fixed on the supporting frame for the non-contact measurement of vertical displacements of piggyback pipelines. The natural frequency of the model pipeline (f_n) and the structural damping factor are obtained by the free-decay test in still water. The flow velocity is measured by an Acoustic Doppler Velocimetry (ADV). The sketch of the configuration of piggyback pipelines is shown in Fig. 2.

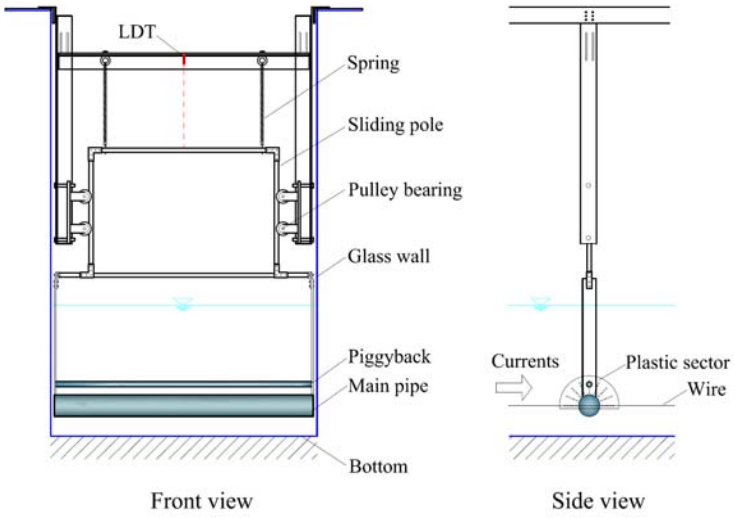

Fig. 1 Details of VIV modeling system

RESULTS AND DISCUSSIONS

Effect of Spacing Ratio *G*/*D*

Effects of the existence of the piggyback on behaviors of the pipeline system are studied under the wall-free condition (e/D = 1.0). Piggyback pipelines with the piggyback installed above the main pipe ($\theta = 90^o$) are simulated first. The spacing ratio between the piggyback and the main pipe (G/D) ranges in 0 ~ 0.5. The natural frequency of the pipeline system is $f_n \approx 0.603$ from the free-decay test. The damping factor is estimated at about 0.067. The mass ratio for the pipeline system is m^* = 1.47. The Reynolds number Re based on the diameter of the main pipe ranges in $0 \sim 6.4\times10^4$.

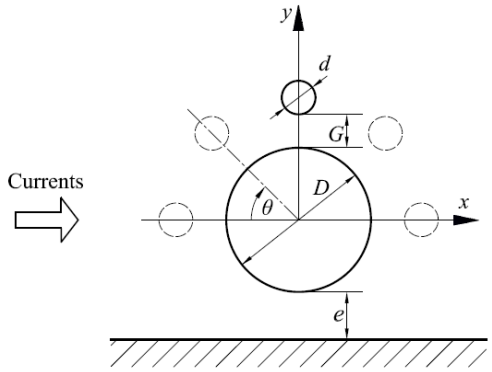

Fig. 2 Configuration of piggyback pipelines

Displacement of piggyback pipeline

Fig.3 shows the time histories of the vertical displacement of vibrating piggyback pipelines for different G/D. The shapes of the vertical displacement curve are much dependent on the value of G/D. Piggyback pipelines are static under the low flow velocity at the initial stage. With the increase of the flow velocity, VIV occurs at a certain instance and then the amplitude of VIV jumps to the maximum value in a very short period. Before the flow velocity reaches the maximum value, vibrations of piggyback pipelines either keep at high amplitudes or decay into low amplitudes depending on the value of G/D. For G/D = 0, namely the piggyback contacting directly above the main pipe, the displacement curve is approximately symmetric about the initial position (y/D =0). For G/D = 0.125, the balance position of the vibrating piggyback pipelines deviates from the initial position with a maximum value of 0.4 D. For G/D = 0.5, the balance position returns back to zero, with the symmetric displacement as that for an isolated pipe ($G/D \approx \infty$). The balance position of the vibrating piggyback pipelines for various values of G/D are shown in Fig. 4(a). The maximum deviation of the balance position from the initial line (y/D = 0) is drawn against G/D in Fig. 4(b). δ and δ_{max} denote the deviation of the balance position from 0 and its maximum value, respectively. With the increase of G/D, δ_{max} increases first (for G/D < 0.25) and then decreases to a small value (for G/D > 0.25). For the medium value of G/D (= 0.125 ~ 0.375), the equilibrium lines of vibrating piggyback pipelines deviate much from the initial position. The maximum deviation occurs at $G/D \approx 0.25$ with a value of $\delta_{max}/D \approx 0.55$. This is

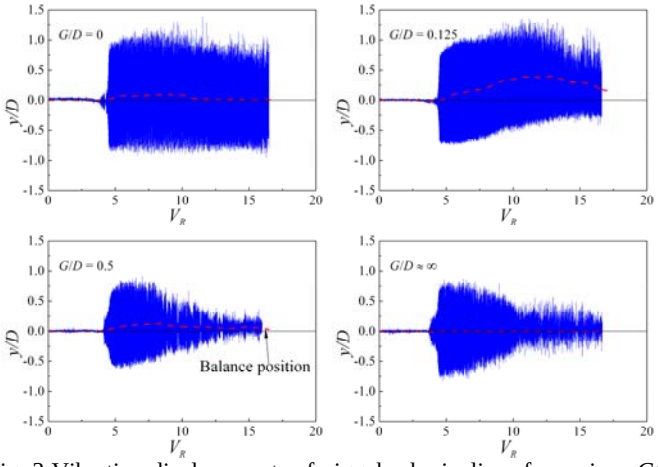

Fig. 3 Vibration displacements of piggyback pipelines for various G/D (e/D = 1.0, $\theta = 90^o$, m^* = 1.47)

because that the wake flows behind the piggyback and the main pipe interfere significantly with each other. The wake flow fields around piggyback pipelines are asymmetric due to the existence of the piggyback, and an upward mean lift force is induced. For the small value of G/D (= 0), the two pipes contact each other and can be treated as an isolated pipe with a larger diameter. For the large value of G/D (≥ 0.5), the two pipes are free from each other, the interference between their wake flows is not significant. The deviation of the balance position for these configurations is small and close to the value for an isolated pipe ($G/D \approx \infty$).

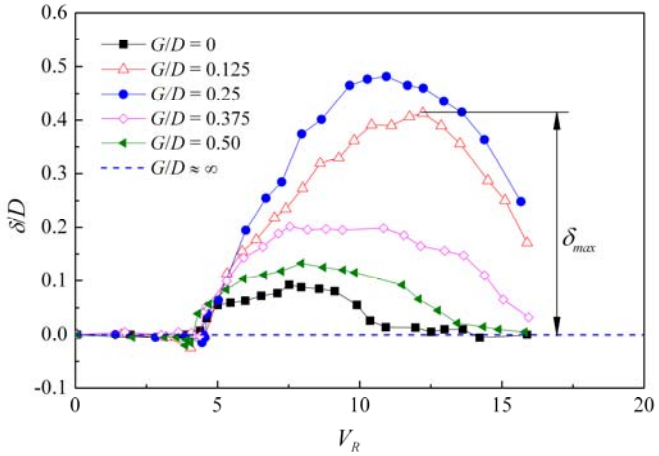

(a)

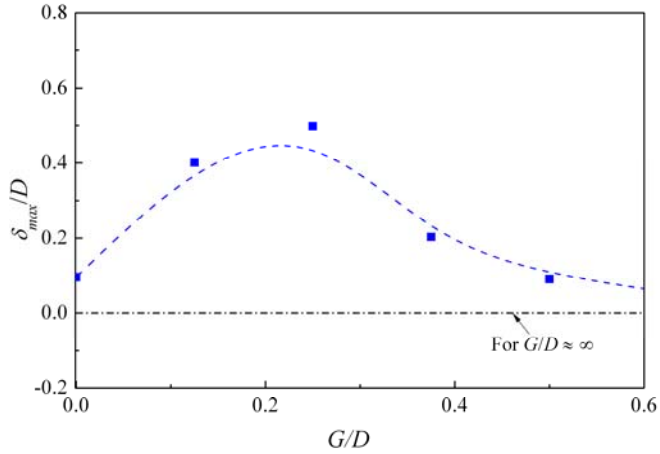

(b)

Fig. 4 (a) Balance positions of vibration for various G/D, (b) maximum deviation of balance position (e/D = 1.0, θ = 90°, m^* = 1.47)

Amplitude and Frequency of VIV

The amplitude and frequency of VIV for piggyback pipelines were analyzed. For wall-free pipelines, the amplitude of VIV is calculated by the difference between the maximum vertical displacement and the balance position. The amplitude of VIV varying with the reduced velocity V_R for different values of G/D are shown in Fig. 5(a). The amplitude of VIV and the "lock-in" range for piggyback pipelines are much dependent on G/D. They generally decrease with the increase of G/D.

According to DNV-RP-105 (2006), the reduced velocity V_R corresponding to A/D = 0.15 has been defined as the critical reduced velocity for onset of VIV ($V_{R,onset}$) and used to calculate the allowable length for spanning pipelines. Here, the same criterion is applied for the definition of $V_{R,onset}$. The values of $V_{R,onset}$ for piggyback pipelines are plotted against G/D in Fig. 5(b). It can been seen that $V_{R,onset}$ is much dependent on G/D. $V_{R,onset}$ is smaller than that for an isolated pipe when G/D = 0. That means that the onset of VIV is more easily to be triggered at the small gap ratio. $V_{R,onset}$ increases with the increase of G/D (for G/D < 0.25), then decreases and tends to be constant when G/D is at a large value (for $G/D \geq 0.5$). The maximum value of $V_{R,onset}$ occurs at $G/D \approx 0.25$, namely the suppression of VIV by the piggyback is most significant at this spacing ratio owing to the interference between the wake flows of two pipes. For the large value of G/D (≥ 0.5), the suppression of VIV by the piggyback is not significant and the value of $V_{R,onset}$ is close to that of an isolated pipe.

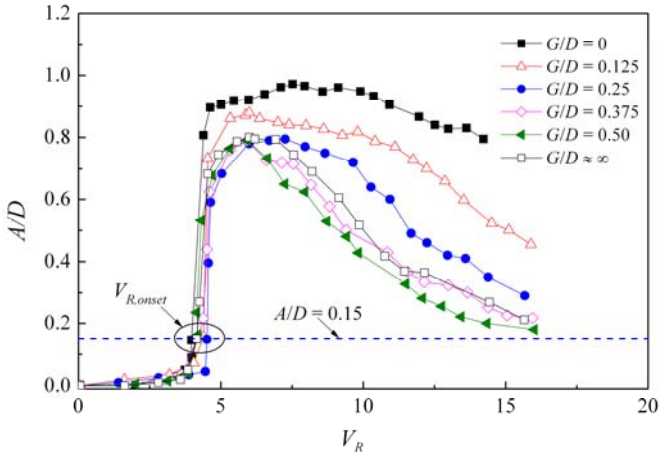

(a)

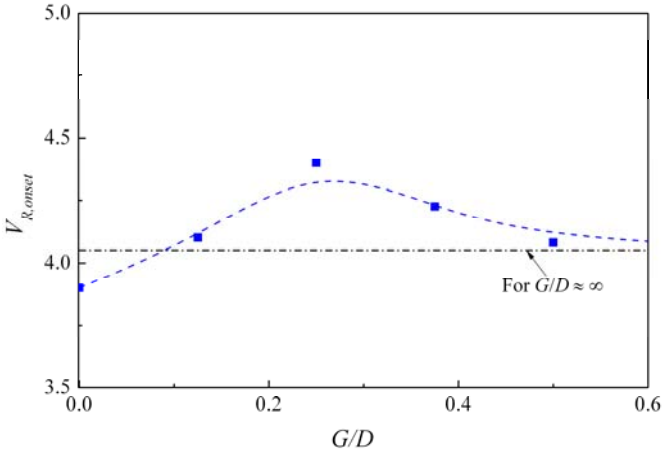

(b)

Fig. 5 (a) Amplitude of VIV vs. V_R for various G/D, (b) critical reduced velocity for onset of VIV varying with G/D (e/D = 1.0, θ = 90°, m^* = 1.47)

Variations of the normalized frequency (f/f_n) of VIV with V_R for various values of G/D are shown in Fig. 6. Generally f/f_n increases with the increase of G/D. At the initial stage of VIV (V_R < 8), the dots for f/f_n are scattered around the Strouhal line ($f/f_n = 0.2V_R$), which is the value of the vortex shedding frequency for a static circular cylinder. It means that the vortex shedding dominates the vibration of piggyback pipelines. Simultaneously, the values of f/f_n are also close to the line of f/f_n = 1.0, namely, there is synchronization between the vortex shedding and the vibration of piggyback pipelines. With the increase of G/D, the dots of

f/f_n deviate from the Strouhal line gradually and have smaller values than it. The values of f/f_n are also much larger than 1.0 owing to the significant interactions between the flow and pipelines at the higher flow velocity. On the one side, the vortex shedding tends to force pipelines vibrating at its frequency; on the other side, piggyback pipelines also tend to keep vibrating at its own natural frequency. Thus the normalized frequency of VIV lies between Strouhal line and unit, a result of the compromise between vortex-induced force and inertia of piggyback pipelines.

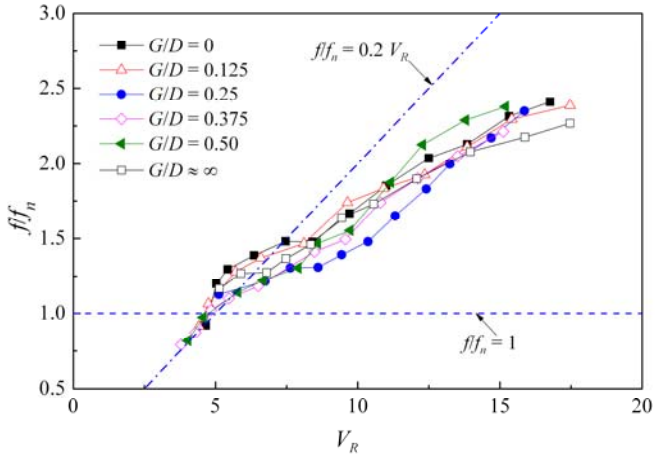

Fig. 6 Normalized frequency of VIV vs. V_R for various G/D (e/D = 1.0, θ = 90°, m^* = 1.47)

Effects of Position Angle θ

In this section, the position angle (θ) of the piggyback relative to the main pipe was changed from 0° to 180° to investigate its effect on the VIV response. The gap ratio G/D was selected at 0.25 here, based on the fact that the most significant suppression of VIV by the piggyback occurs around this gap ratio for θ = 90° (see Fig. 5(b)).

Displacement of piggyback pipeline

Fig.7(a) shows the time histories of the vertical displacement of piggyback pipelines with different position angle. It can be seen that the responses of piggyback pipelines are quite different for the different values of θ. For θ = 0°, namely the piggyback in tandem with the main pipe, the displacement curve is approximately symmetric about the initial position (y/D = 0), only a slight deviation when V_R > 15. For θ = 30°, the deviation of the balance position increases with the increase of V_R, while the VIV of piggyback pipelines only occurs in a narrow range of V_R. For θ = 90°, the deviation of the balance position and the amplitude of VIV all are at large values. For θ = 135°, the whole pipeline system rises up with the increase of V_R, while there is no significant vibration of pipelines in the process of increasing the flow velocity. The balance positions of vibrating piggyback pipelines for various values of θ are plotted in Fig. 7(b). It can be seen that the balance position varies much with θ. For the tandem configurations of two pipes (θ = 0° and 180 °), the balance position of vibrations are almost close to 0, only with small deviation from the initial position at the large reduced velocity. This is because that the mean lift force on pipelines is close to zero for these symmetric pipeline configurations about the horizontal center line. For other position angles, the balance position all are above the initial position and the deviation generally increases with the increase of V_R. This is because that the existence of the piggyback induces an upward lift force on the pipeline system. The mean lift force also increases with the increase of V_R. The maximum values of the deviation occur at θ = 30° and 135°, respectively, which can be explained by the maximum mean lift forces occur at these two position angles.

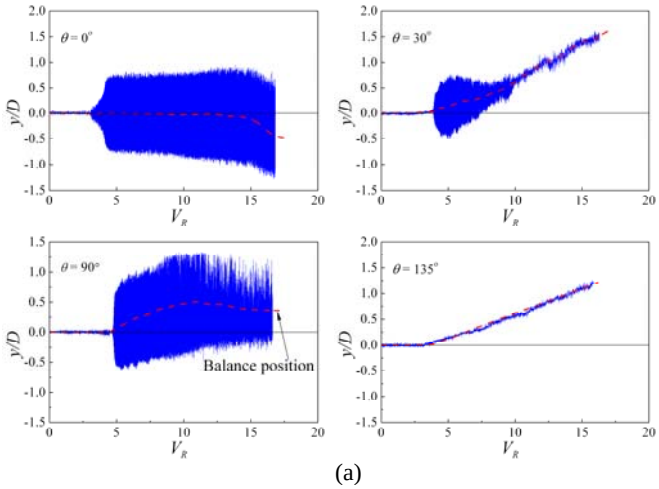

(a)

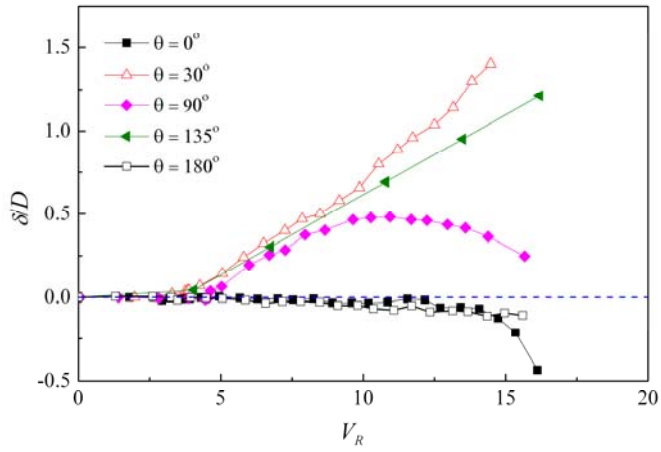

(b)

Fig. 7 (a) Vibration displacements of vibrating piggyback pipelines for various θ, (b) balance position of vibration for various position angle (e/D = 1.0, G/D = 0.25, m^* = 1.47)

Amplitude and Frequency of VIV

Amplitudes of VIV varying with the reduced velocity V_R for different values of θ are shown in Fig. 8(a). It can be seen that the curves for θ = 0°, 90° and 180 ° have large amplitudes and wide "lock-in" ranges, while those for θ = 30° has the smaller amplitude and narrow "lock-in" range, even for θ = 135°, there is no evident vibration occurring. The maximum amplitude occurs at θ = 0° with a value up to A/D = 0.95.

Variation of the normalized frequency (f/f_n) of VIV with V_R for various values of θ is shown in Fig. 8(b). Generally, f/f_n increases with the increase of V_R. At the initial stage of VIV (V_R < 6), the values of f/f_n don't varies much with θ. The dots for f/f_n are focused around the Strouhal line (f/f_n = 0.2V_R), which means that the vortex shedding dominates the vibration of piggyback pipelines. The values of f/f_n are also close to the line of f/f_n = 1.0 at the initial stage. With the increase of V_R (for V_R > 6), the position angle has significant effect on the frequency of VIV. The dots of f/f_n cover the area between the Strouhal line and the line of f/f_n = 1.0. For θ = 120°, f/f_n is very close to the Strouhal line in the testing velocity range and has the highest vibrating

frequency among these position angles. That means that the vortex shedding dominates the frequency of VIV. For θ = 180°, the value of f/f_n has the lowest vibrating frequency, which means that piggyback pipelines keep vibrating at its own natural frequency.

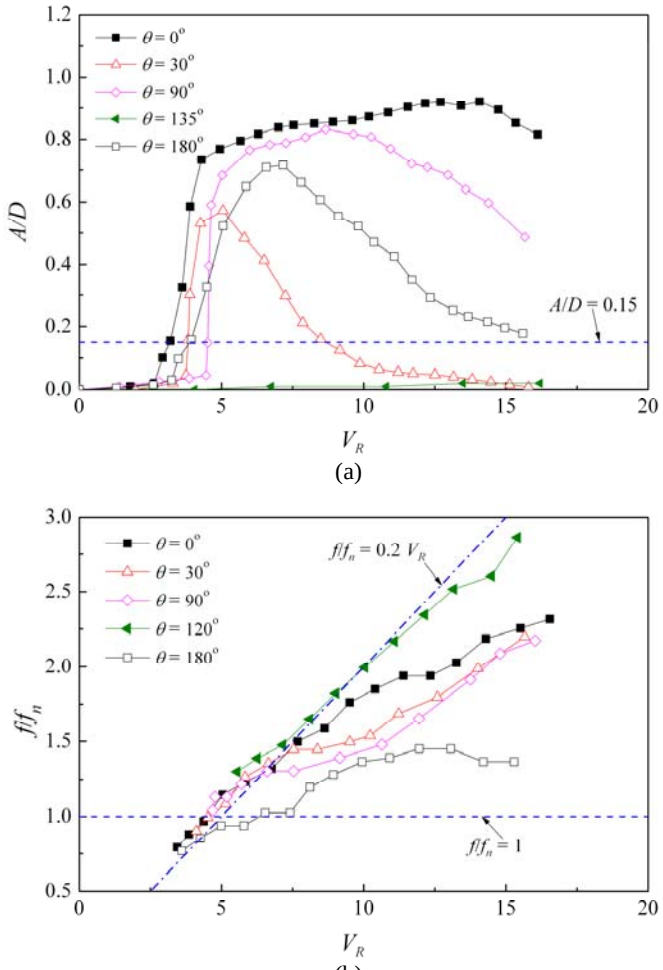

Fig. 8 (a) Amplitude of VIV vs. V_R for various position angle, (b) normalized frequency of VIV vs. V_R for various position angle (e/D = 1.0, G/D = 0.25, m^* = 1.47)

Effects of Mass Ratio *m**

Here, VIV responses of piggyback pipelines were further simulated with three mass ratios, namely, m^* = 1.18, 1.32 and 1.47. The mass ratio of pipelines was changed by adjusting the quantity of aluminium blocks filled in the main pipe. The piggyback is installed vertically above the main pipe with a spacing ratio G/D = 0.5.

Fig. 9(a) shows the amplitude of VIV varying with V_R for three mass ratios. It can be seen that the maximum A/D and the band width of synchronization generally decrease with the increase of m^*. This is mainly because for the smaller mass ratio m*= 1.18, the density of the water flow and the pipe is very close, the interactions between water and pipelines is more significant. For the critical reduced velocity, there is distinct difference among these three mass ratios. $V_{R,onset}$ increases with the decrease of m^*. The normalized frequency of VIV is plotted against V_R in Fig. 9(b). The mass ratio has little effect on the frequency of VIV. f/f_n increases with the increase of V_R, and the symbols for f/f_n are scattered between the lines for $f/f_n = 0.2V_R$ and f/f_n = 1.0, and a little closer to the Strouhal line.

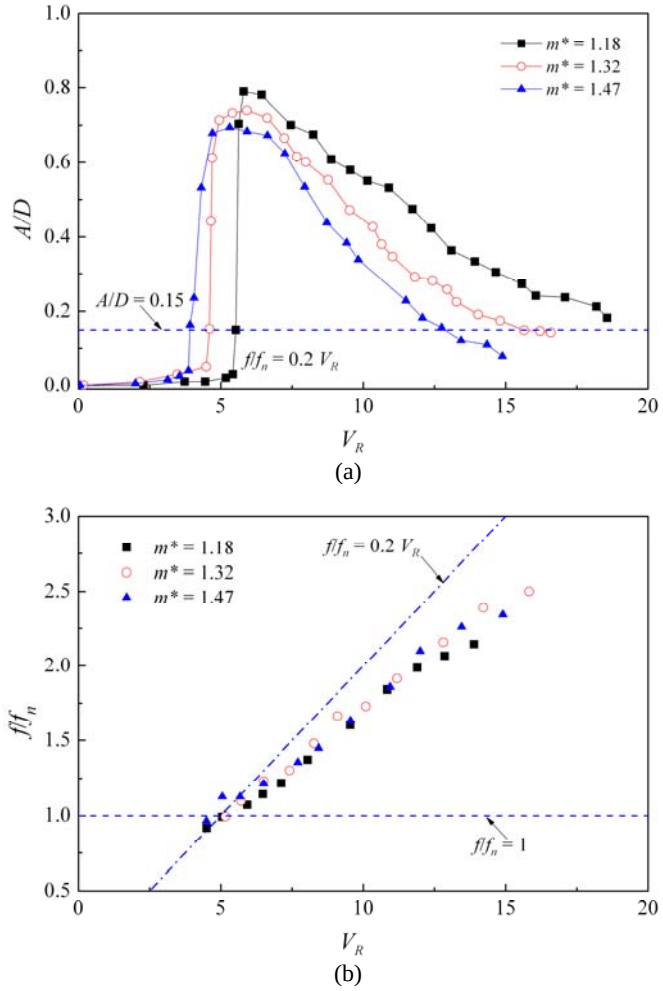

Fig. 9 (a) Amplitude of VIV vs. V_R for different mass ratio, (b) normalized frequency of VIV vs. V_R for different mass ratio (e/D = 1.0, G/D = 0.5, θ = 90°)

CONCLUSIONS

Transverse VIV for spanning piggyback pipelines under the steady current was physically modeled in a water flume. In each test, the flow velocity was increased gradually from 0 to 0.8m/s, corresponding to a reduced velocity ranging from 0 to 16, which covers the typical range of the reduced velocity for pipelines in field conditions. The effects of the configuration parameters, including the spacing ratio (G/D), the position angle (θ) and the mass ratio (m^*), on the equilibrium position of VIV (δ/D), the critical reduced velocity for onset of VIV ($V_{R,onset}$), the normalized amplitude (A/D) and frequency (f/f_n) of VIV are investigated. The conclusions are listed as following:

(1) The maximum deviation of the balance position and the maximum critical reduced velocity for onset of VIV occur at the spacing ratio $G/D \approx 0.25$.

(2) The maximum deviation of the equilibrium line occurs at $\theta \approx 30°$ and 135°. The amplitudes of VIV at position angles θ around 30° and 135° are smaller than that for an isolated pipe, even there is no evident VIV occurring at θ = 135°.

(3) The amplitude of VIV and the "lock-in" range decreases with the increase of mass ratio. The mass ratio has little effect on the frequency of VIV.

ACKNOWLEDGEMENTS

This work is financially supported by National Natural Science Foundation of China (Grant No. 51109202) and the Open Foundation of the Key Laboratory of Port, Waterway and Sedimentation Engineering of Ministry of Transport.

REFERENCES

An, HW, Cheng, L, and Zhao M (2008). "Numerical Simulation of Vortex-Induced Vibration of Two Circular Cylinders of Different Diameters." *Proc 18th Int Offshore and Polar Eng Conf*, Vancouver, ISOPE, Vol 3, pp 264-271.

Chung, JS, Whitney, AK, Lezius, D, and Conti, RJ (1994). "Flow-induced torsional moment and vortex suppression for a circular cylinder with cables." *Proc 4th Int Offshore and Polar Eng Conf*, Osaka, ISOPE , Vol 3, pp 447–459.

Det Norske Veritas (2006). "Free spanning pipelines." Recommended practice DNV-RPF105.

Gao, FP, Yang, B, Wu, YX, and Yan, SM (2006). "Steady current induced seabed scour around a vibrating pipeline." *Applied Ocean Research*, Vol 28, pp 291–298.

Kalahatgi, SG, and Sayer PG (1997). "Hydrodynamic forces on piggyback pipeline configurations." *J Waterway, Port, Coastal and Ocean Eng*, Vol 123, No 1, pp 16–22.

Kamarudin, MH, Thiagarajan, KP, and Czajko, A (2006). "Analysis of current-induced forces on offshore pipeline bundles." *5th Int Conf Computational Fluid Dynamics in the Process Industries*, Melbourne, Vol 1, pp 1–6.

Li, YC, and Zhang, NC (1994). "The hydrodynamic characteristic of submarine piggyback pipeline in wave-Current coexisting Field." *Proc 4th Int Offshore and Polar Eng Conf*, Osaka, ISOPE , Vol 2, pp 10–15.

Rahmanian, M, Zhao, M, Cheng L, and Zhou, TM (2012). "Two-degree-of-freedom vortex-induced vibration of two mechanically coupled cylinders of different diameters in steady current." *J Fluids and Structures*, Vol 35, pp 133–159.

Zang, ZP, Gao, FP, and Cui, JS (2012). "Vortex Shedding and Vortex-Induced Vibration of Piggyback Pipelines in Steady Currents." *Proc 22th Int Offshore and Polar Eng Conf*, Rhodes, ISOPE, Vol 3, pp 565-571.

Zhao, M, Cheng, L, Teng, B, and Dong GH (2007a). "Hydrodynamic forces on dual cylinders of different diameters in steady currents." *J Fluids and Structures*, Vol 23, No 1, pp 59–83.

Zhao, M, Cheng, L, and Teng, B (2007b). "Numerical modeling of flow and hydrodynamic forces around a piggyback pipeline near the seabed." *J Waterway, Port, Coastal and Ocean Eng*, Vol 133, No 14, pp 286–295.